Beyond π–π Stacking: Understanding Inversion Symmetry Breaking in Crystalline Racemates

Yiran Wang, Matthew Nisbet, Kendall Kamp, Emily Hiralal, Romain Gautier, P. Shiv Halasyamani, Kenneth Poeppelmeier

Beyond π-π Stacking: Understanding Inversion Symmetry Breaking in Crystalline Racemates

Yiran Wang,[†] Matthew L. Nisbet,[†] Kendall R. Kamp,[†] Emily Hiralal,[†] Romain Gautier,[‡] P. Shiv Halasyamani,[‖] and Kenneth R. Poeppelmeier*,[†]

[†]Department of Chemistry, Northwestern University, 2145 Sheridan Road, Evanston, Illinois 60208, USA

[‡]Institut des Matériaux Jean Rouxel (IMN), Université de Nantes, CNRS, F-44000 Nates cedex 3, France

[‖]Department of Chemistry, University of Houston, 112 Fleming Building, Houston, Texas 77204-5003, United States

ABSTRACT: The design of noncentrosymmetric (NCS) solid state materials, specifically, how to break inversion symmetry between enantiomers, has intrigued chemists, physicists, and materials scientists for many years. Because the chemical complexity of molecular racemic building units is so varied, targeting these materials is poorly understood. Previously, three isostructural racemic compounds with a formula of $[Cu(H_2O)(bpy)_2]_2[MF_6]_2{\cdot}2H_2O$ (bpy = 2,2'=bipyridine; M = Ti, Zr, Hf) were shown to crystallize in the NCS space group *Pna*2$_1$, of polar, achiral crystal class *mm*2. In this work, we synthesized five new racemic compounds with a formula $[Cu(H_2O)(dmbpy)_2]_2[MF_6]_2{\cdot}xH_2O$ (dmbpy = 4,4'/5,5'-dimethyl-2,2'-bipyridine; M = Ti, Zr, Hf). Single crystal X-ray diffraction reveals that the five newly synthesized compounds feature equimolar combinations of Δ- and Λ-$Cu(dmbpy)_2(H_2O)^{2+}$ complexes that are assembled into similar packing motifs of those found in the reported NCS structure, but all crystalize in centrosymmetric (CS) space groups. Seven structural descriptors were created to analyze the intermolecular interactions on the assembly of Cu racemates in the CS and NCS structures. The structural analysis reveals that in the CS structures, the inversion center results from parallel heterochiral *π*-*π* stacking interactions between adjacent Cu racemates regardless of cation geometries, hydrogen bonding networks, or interlayers architectures, whereas in the NCS structure, nonparallel heterochiral *π*-*π* interactions between the adjacent Cu racemates precludes the inversion center. The parallel heterochiral *π*-*π* interactions in the CS structures can be rationalized by the restrained geometries of the methyl-substituted ligands. This work demonstrates that the introduction of nonparallel stacking can suppress the formation of an inversion center for a NCS racemate. A conceptual framework and practical approach linking the absence of inversion symmetry in racemates is presented for all NCS crystal classes.

Introduction

The rational design of materials calls for a deep understanding of how atoms, units, or motifs in a crystal structure pack together. Noncentrosymmetric (NCS) solids, in which an inversion center is absent in the structure, are known to display a wide range of functional properties such as nonlinear optical activity, piezoelectricity, ferroelectricity and pyroelectricity.[1–3] Functional building units (FBUs), such as polar early transition-metal (ETM) octahedra,[4–9] borate clusters,[10–12] poly-anions,[13–15] and π-conjugated units,[16,17] are great sources from which to construct NCS solids with superior properties. However, inversion symmetry is often favorable during crystallization for its efficiency in close packing of the basic building units (BBUs),[18,19] and the challenges for synthesizing new NCS solids arises from aligning the FBUs without an inversion center. To direct a NCS structure, one efficient strategy is to introduce chiral BBUs since they do not possess an inversion center by nature. Solids with enantiomerically-pure chiral BBUs are guaranteed to crystalize in the NCS chiral crystal classes because chiral BBUs with the same handedness can be related by proper symmetry operations (translations, rotations, and combinations of these), but such solids often require enantiomeric purification, which complicates the synthetic process.

An alternative method to craft NCS solids with chiral BBUs is to combine enantiomers of both handedness and form racemates.[20–23] Although enantiomers with the opposite handedness can be related by an inversion center and crystallize into CS racemates, it is still possible to form NCS racemates with enantiomers of both handedness. Such formations requires the enantiomers to relate to one another by symmetry elements such as (i) mirror/glide planes, (ii) rotoinversions, (iii) dihedral rotations, and (iv) principle rotations (**Erreur ! Source du renvoi introuvable.**re 1).[20,22] When the enantiomers are related by mirror/glide planes or rotoinversion, the solid will form an achiral racemic compound, a single phase which is composed of equimolar enantiomers with the opposite handedness. When the enantiomers are related only by dihedral rotations and/or principle rotations, the solid will be chiral and form either racemic conglomerates—a mechanical mixture of enantiomorphic crystals that each of crystal contains a single enantiomer[24]–or kryptoracemates—an extremely rare chiral crystal which contains enantiomers with opposite handedness that are symmetrically independent to

each other.[25,26] In fact, it is not uncommon to find racemates in NCS crystals; for example, a manual screening of NCS organic crystals with mirror symmetry identified 632 racemates (16.5%) in the Cambridge Structural Database.[27] However, it still remains unclear how to break inversion symmetry between racemic BBUs at molecular level, bringing challenges to design new NCS racemates on a rational basis.[28,29]

Recently, Δ/Λ-Cu(bpy)$_2$(H$_2$O)$^{2+}$ complexes have been found to crystalize in the polar and achiral NCS space group *Pna*2$_1$ with polar anions MF_6^{2-} (M = Ti, Zr, Hf; bpy = 2,2′ -bipyridine).[21,23] Owing to second-order Jahn–Teller effects and hydrogen bonding network, MF_6^{2-} octahedra undergo an out-of-center distortion and are aligned by a

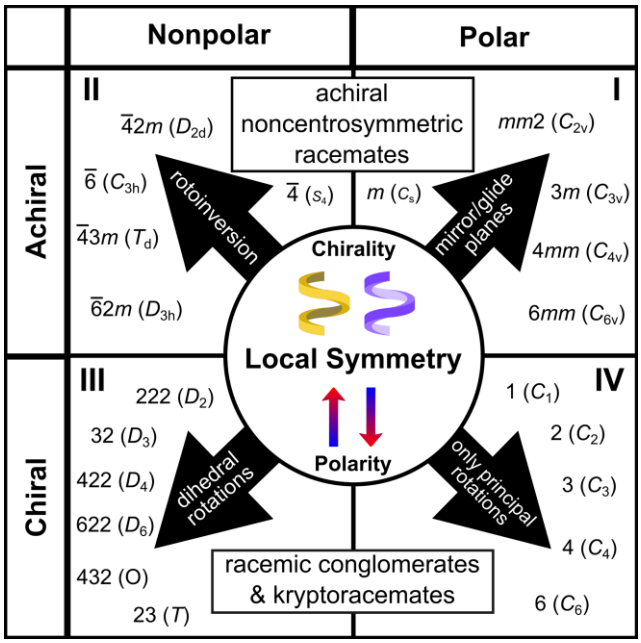

Figure 1. A road map for NCS racemates. The yellow and purple swirls represent enantiomers with the opposite handedness and the arrows represent the symmetry elements that relates the chiral BBUs.

screw axis, giving an overall polar moment. This NCS polar racemic structure (referred to NCS-Cu/bpy/M hereafter) is unique, and is one of the 4 NCS crystal structures out from 14 crystal structures that contain equimolar Δ/Λ-Cu(bpy)$_2$(H$_2$O)$^{2+}$ BBUs in the Cambridge Structural Database (CSD version 5.42 from March 2022), while the other NCS examples are compounds with multicomponent BBUs and complex motifs.[30–32] To further understand the chemical origins of inversion symmetry breaking in the NCS-Cu/bpy/M structure, we utilized bpy's derivatives with methyl-substituents, dmbpy (dmbpy = 4,4'/5,5'-dimethyl-2,2'-bipyridine) ligands, to perturb the coordination environment of the enantiomers and synthesized five new compounds with equimolar Δ/Λ- Cu(dmbpy)$_2$(H$_2$O)$^{2+}$ cations and MF_6^{2-} anions. We created a series of structural descriptors to compare the structures and analyze intermolecular interactions of the reported NCS and newly synthesized CS compounds. Through a detailed structural analysis, parallel heterochiral π–π interactions are identified as the key factor in the formation of the inversion center between the adjacent Cu enantiomers, providing insights for the rational design of new NCS racemic materials.

Methods

Caution: Hydrofluoric acid (HF) is toxic and corrosive! HF must be handled with extreme caution and with the appropriate protective gear.

Materials

TiO$_2$ (Aldrich, 99.9+%), ZrO$_2$ (Alfa Aesar, 99.978%), HfO$_2$ (Aldrich, 98%), CuO (SigmaAldrich, ≥99.0%), 5,5′ -Dimethyl-2,2′ -dipyridyl (Fisher Scientific, ≥98.0%), 4,4′ -Dimethyl-2,2′ -dipyridyl (SigmaAldrich, 99%), HF(*aq*) (Sigma-Aldrich, 48% wt. in H$_2$O, ≥99.99+% trace metals basis) were used as received. Reagent amounts of deionized water were used.

Hydrothermal Synthesis

The compounds reported here were synthesized via the hydrothermal pouch method.[33] In each reaction, reagents were heat-sealed in Teflon pouches. Groups of six pouches were then placed into a 125 mL Parr autoclave with 40 mL deionized water as backfill. The autoclave was heated at a rate of 5 °C/min to 150 °C and held at 150 °C for 24 h. The autoclaves were allowed to cool to room temperature at a rate of 6 °C/h. Solid products were recovered by vacuum filtration.

Compound **1**, [Cu(5dmbpy)$_2$(H$_2$O)][TiF$_6$]·H$_2$O was synthesized in a pouch containing 0.4195 mmol CuO, 0.4195 mmol TiO$_2$, 0.835 mmol 5dmbpy, 0.05 mL (1.38 mmol) HF(aq), and 0.2 mL (11 mmol) H$_2$O. Greenish blue crystals (compound **1**) were recovered by vacuum filtration with other unknown phases.

Compound **2**, [Cu(5dmbpy)$_2$(H$_2$O)][ZrF$_6$]·1.5H$_2$O was synthesized in a pouch containing 0.4195 mmol CuO, 0.4195 mmol ZrO$_2$, 0.835 mmol 5dmbpy, 0.15 mL (4.14 mmol) HF(aq), and 0.1 mL (5.5 mmol) H$_2$O. Greenish blue crystals (compound **2**) were recovered by vacuum filtration with a small amount of other unknown phases.

Compound **3**, [Cu(5dmbpy)$_2$(H$_2$O)][HfF$_6$]·1.09H$_2$O was synthesized in a pouch containing 0.4195 mmol CuO, 0.4195 mmol HfO$_2$, 0.835 mmol 5dmbpy, 0.15 mL (4.14 mmol) HF(aq), and 0.1 mL (5.5 mmol) H$_2$O. Greenish blue crystals (compound **3**) were recovered by vacuum filtration with a small amount of other unknown phases.

Compound **4**, [Cu(4dmbpy)$_2$(H$_2$O)][ZrF$_6$]·2.5H$_2$O was synthesized in a pouch containing 0.4195 mmol CuO, 0.4195 mmol ZrO$_2$, 0.835 mmol 4dmbpy, 0.15 mL (4.14 mmol) HF(aq), and 0.1 mL (5.5 mmol) H$_2$O. Blue crystals (compound **4**) were recovered by vacuum filtration with other unknown phases.

Compound **5**, [Cu(4dmbpy)$_2$(H$_2$O)][HfF$_6$]·1.09H$_2$O was synthesized in a pouch containing 0.4195 mmol CuO, 0.4195 mmol HfO$_2$, 0.835 mmol 5dmbpy, 0.15 mL (4.14 mmol) HF(aq), and 0.1 mL (5.5 mmol) H$_2$O. Blue crystals

(compound **5**) were recovered by vacuum filtration with a small amount of other unknown phases.

Single-Crystal X -ray Diffraction

A suitable single crystal was mounted on a glass fiber with paratone oil and the intensity data of the single crystal were collected at 100 K on an XtaLAB Synergy diffractometer equipped with a micro-focus sealed X-ray tube PhotonJet (Mo) X-ray source and a Hybrid Pixel Array Detector (HyPix) detector. Temperature of the crystal was controlled with an Oxford Cryosystems low-temperature device. Data reduction was performed with the CrysAlisPro software using an numerical absorption correction.[34] The structure was solved with the ShelXT,[35] using Intrinsic Phasing as implemented in Olex2.[36] The model was refined with ShelXL using least squares minimization. The structures were checked for missing symmetry with PLATON.[37]

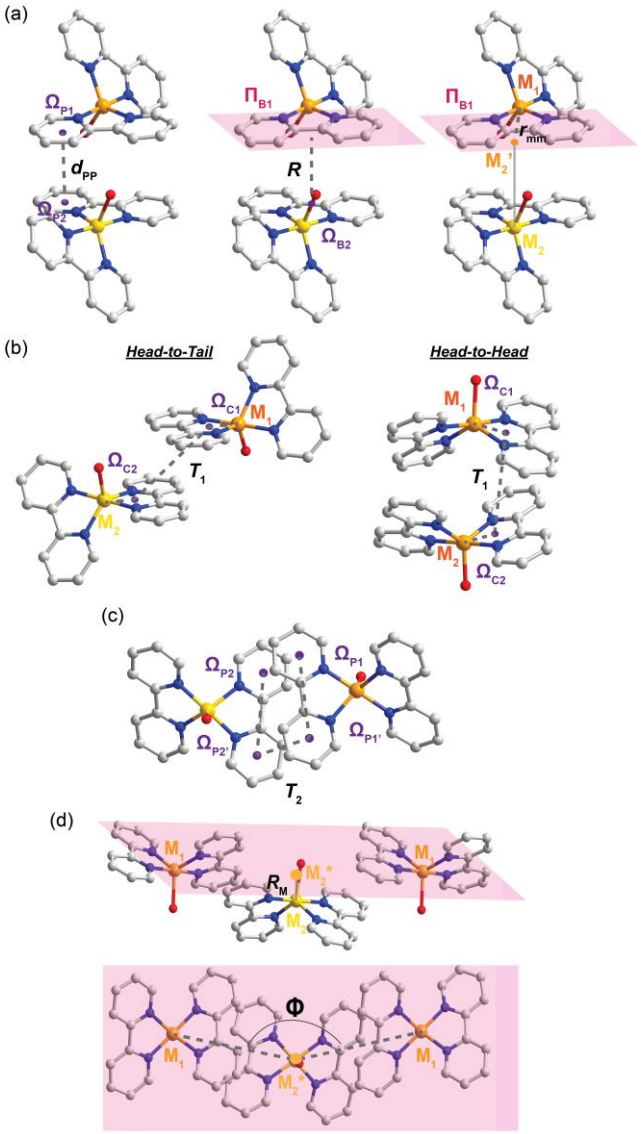

Figure 2. Illustration of descriptors (a) distance d_{PP} (left), R (middle) and r_{mm} (right), torsion angles (b) T_1 and (c) T_2. (d) The illustration of descriptors distance R_M (up) and angle Φ (down). The examples are taken from the reported compound $[Cu(H_2O)(bpy)_2]_2[TiF_6]\cdot 2H_2O$.

Structural Descriptors

In order to quantify the intermolecular interactions between the ligands in the Cu complexes, we have introduced the following descriptors adopted from a published work by Petrović et al.[38] The stacking interactions between the adjacent bpy ligands can appear between C_5N-aromatic rings and are described with distances d_{PP}, R and r_{mm}, (Figure 2a) and torsion angles T_1 (Figure 2b) and T_2 (Figure 2c). The three distances represent the displacements of the interacting ligands from the three directions. Distance d_{PP} is the shortest distance between centroids of two pyridine fragments (Ω_{P1} and Ω_{P2}) from the adjacent interacting ligands. Distance R is the distance from the centroid of ligand of the second complex (Ω_{B2}) to the average plane including the interacting ligand of the first complex (Π_{B1}). Distance r_{mm} is the distance from the metal ion of the first complex (M_1) to the projection of the metal ion of the second complex onto Π_{B1} (M_2'). Torsion angle T_1 represents the relative direction of the interacting ligands. Torsion angle T_1 is defined as the M_1–Ω_{C1}–Ω_{C2}–M_2 angle, and Ω_{C1} and Ω_{C2} are defined as the centroids of the chelate rings from the first and second complexes, respectively. When T_1 falls between 0° and 90°, the two interacting ligands tend to head in the same direction and are *head-to-head* oriented. Otherwise, when T_1 falls between 90° and 180°, the two interacting ligands tend to head in opposing directions and are *head-to-tail* oriented. Torsion angle T_2 represents the stacking arrangements between the interacting ligands and is defined as the Ω_{P1}–$\Omega_{P1'}$–$\Omega_{P2'}$–Ω_{P2} angle. If T_2 is smaller than 90°, it indicates both C_5N-aromatic rings from the ligands overlap, and conversely, if T_2 is larger than 90°, it indicates only one C_5N-aromatic rings from each ligand overlap. When T_2 is 0° or 180°, the two ligands are aligned parallel, and their geometry corresponds to *parallel* packing. Otherwise, the two ligands are aligned with an angle and their geometry corresponds to *nonparallel* packing.

To describe the arrangement of the Cu enantiomers in the racemic chains of the compounds discussed, we have developed two descriptors, R_M and Φ parameters, for measuring the offset of BBUs (Figure 2d). Distance R_M is the normal distance from the Cu atom of the enantiomer with up orientation (M_2) to the average plane including all the Cu atom of the enantiomer with down orientation (M_1) in a certain racemic chain. The angle Φ is defined as M_1–M_2*–M_1 where M_2* is the projection of M_2 onto the average plane of M_1. The R_M and Φ parameters present the offset of the racemates perpendicular to and along the chain direction.

Results

Structure Descriptions

In order to investigate how steric effects influence racemates' crystal packing, we introduced methyl groups on 2,2′ -bipyridyl ligands and examined two distinct substituent positions where one is on the 5,5'-position while the other is on the 4,4'-position. By exploring the synthesis of CuO, MO_2 / dmbpy / HF(aq) (M = Ti, Zr, Hf; dmbpy = 4,4′ -dimethyl-2,2′ -dipyridyl, 5,5′ -dimethyl-2,2′ -dipyridyl), we

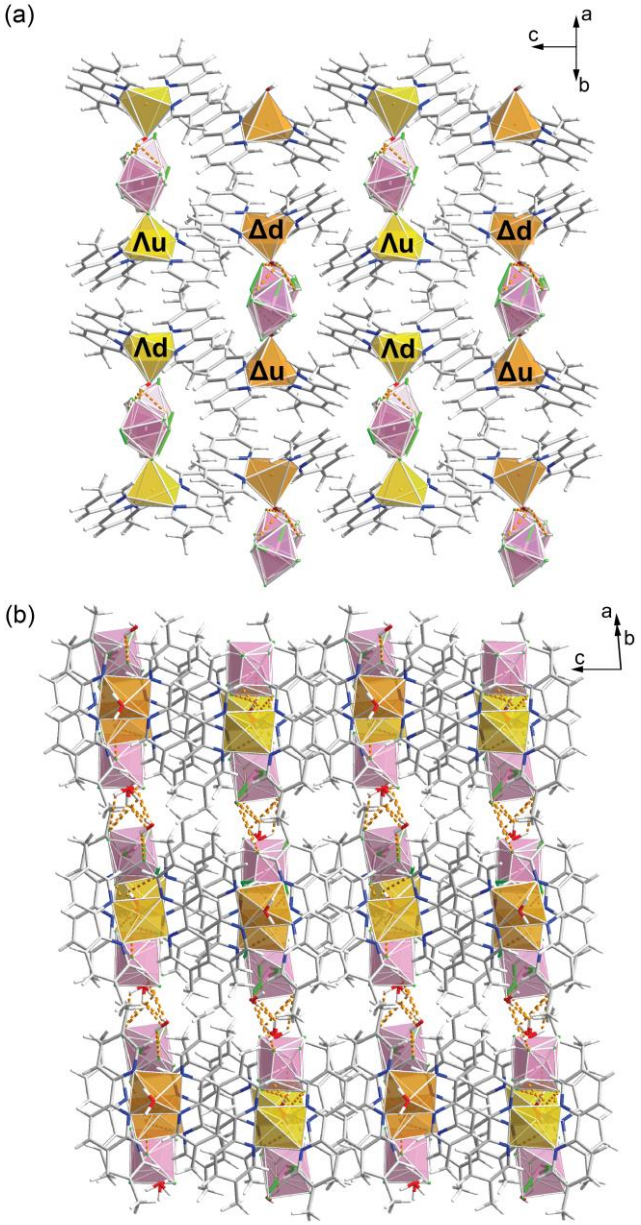

Figure 3. (a) Racemic layer of **1** view against *c* axis. (b) Crystal structure of **1** view against *c* axis (this view is produced from Figure 3a by 90° rotation around horizontal direction). Orange, blue, red, grey, and white spheres represent Cu, N, O, C, and H atoms, respectively. Yellow, orange, and pink polyhedra represent Cu-centered cations with Λ- and Δ- configurations and Ti-centered anions, respectively. The orange dashed line represent hydrogen bonds.

discovered three compounds based on racemic combinations of Δ/Λ-Cu(5dmpy)$_2$(H$_2$O)$^{2+}$ cations and MF$_6^{2-}$ anions (namely compounds **1**, **2** and **3**) and two compounds based on combinations of chiral Δ/Λ-Cu(4dmpy)$_2$(H$_2$O)$^{2+}$ cations and MF$_6^{2-}$ anions (namely compounds **4** and **5**). The crystallographic information is summarized in Tables S1-2.

Compound **1** has the formula [Cu(5dmbpy)$_2$(H$_2$O)]$_2$[TiF$_6$]$_2$·2H$_2$O and crystallizes in the space group $P\bar{1}$. The asymmetric unit of **1** contains two chiral Cu(5dmbpy)$_2$(H$_2$O)$^{2+}$ cations with the same handedness but different orientations, two positionally disordered TiF$_6^{2-}$ anions and two free water molecules with one being positionally disordered. The Cu enantiomers with the opposite handedness (Λu/Δd and Λd/Δu) are generated by an inversion center and the two sets of racemic Δ/Λ-Cu(5dmbpy)$_2$(H$_2$O)$^{2+}$ cations display C_2 symmetry. The angle between the copper atom and centroids of the two ligands in the cations are slightly different between the two sets, with one being 141.01° and the other being 137.15° (Figure S1). To examine the geometry of the cations, the τ_5 parameter ($\tau_5 = \frac{\beta-\alpha}{60^\circ}$) was used where β and α represent the largest and second largest bond angles.[39] The value of τ_5 parameter indicates the shape of the five-vertex polyhedron formed by the molecule; when τ_5 = 0, the shape is a square pyramid, while τ_5 = 1 indicates a triangular bipyramid. For the Cu cations in **1**, τ_5 values are 0.90/0.87, indicating that the shapes of the cations are close to triangular bipyramidal. Two racemic chains are formed via heterochiral *π*-*π* stacking interactions between Cu enantiomers with the opposite handedness and run along the *c* axis with the arrangements of Λd–Δu–Λd–Δu and Λu–Δd–Λu–Δd (u = up and d = down describe the orientation of these cations along the *b** direction). Then, the chains are extended into layers by altering the arrangements and stacking Cu enantiomers with the same handedness via homochiral *π*-*π* stacking interactions (Figure 3a). The TiF$_6^{2-}$ anions are in the voids created within layers of homochiral enantiomers, forming hydrogen bonds with the bound water on the cations. Each TiF$_6^{2-}$ anion participates in hydrogen bonding with ligated water on two Cu enantiomers of same handedness, and as a result, Ti—F bond lengths vary from 1.831(2) to 1.908(3) Å. The differences in bond lengths lead to a small out of center distortion in the TiF$_6^{2-}$ octahedron but the overall centrosymmetry of the crystal cancels the polar moment between TiF$_6^{2-}$ anions. Finally, the layers stack in three dimensions in an eclipsed manner through a weaving-shape intermolecular hydrogen bond network between the TiF$_6^{2-}$ anions and free waters (Figure 3b).

Compound **2** has the formula $[Cu(5dmbpy)_2(H_2O)]_2[ZrF_6]_2 \cdot 2.5H_2O$ and crystallizes in the space group $P\bar{1}$. Similar to **1**, the asymmetric unit of **2** also contains two $Cu(5dmbpy)_2(H_2O)^{2+}$ cations with the same handedness but different orientations, two ZrF_6^{2-} anions and three free water molecules; all the anions and the free water molecules are positionally ordered in **2**. The Cu cations in **2** also appear with C_2 symmetry with the angles between the Cu atom and the centroids of ligands being 150.90° and 145.26° (Figure S2). The calculated τ_5 values are 0.83 and 0.80 for each independent Cu cations in **2**, indicating a triangular bipyramidal geometry for both. The ZrF_6^{2-} anions connect to the free water and the bound water of Cu cations through hydrogen bonding, giving rise to a slightly distorted octahedra with Zr—F bond lengths varying from 1.9887(13) to 2.0235(12) Å. The overall dipole moment of the anions is counteracted by the centrosymmetry of the crystal. The layer packing pattern of **2** is comparable to **1**. Cu enantiomers with the opposite handedness arrange in Λd–Δu–Λd–Δu and Λu–Δd–Λu–Δd chains (u = up and d = down describe the orientation of these cations along the *b* direction) along *c* axis via heterochiral *π*-*π* stacking interactions and the chains pack into layers along the *b* axis via homochiral *π*-*π* stacking (Figure 4a). The disparity between **1** and **2** is the interlayer stacking. In **2**, a different waving-shape hydrogen bonding network leads to an interlayer architecture in a staggered manner rather than an eclipsed manner along the *a* axis (Figure 4b).

Compound **3** has the formula $[Cu(5dmbpy)_2(H_2O)]_2[HfF_6]_2 \cdot 2.1H_2O$ and is isostructural to **2** except for slightly different free water positions and occupancies. The angles between the Cu atom and the centroids of the ligands are 149.19/145.13° and τ_5 values for the Cu complexes are 0.83/0.84 in **3**. The anions are minorly distorted and Hf—F bond lengths vary from 1.970(3) to 2.019(3) Å.

Compound **4** has the formula $[Cu(4dmbpy)_2(H_2O)]_2[ZrF_6]_2 \cdot 7H_2O$ and crystallizes in the space group $P2_1/c$. Similar to the aforementioned compounds, the asymmetric unit of **4** contains two $Cu(4dmbpy)_2(H_2O)^{2+}$ cations with same handedness but different orientations, two unique ZrF_6^{2-} anions and five free water molecules. However, the symmetry of the Cu cations is reduced to C_1 owing to the large tilt of the apical bound water ligand. Similar symmetry reduction in five-coordinated Cu complexes were also reported in compounds with $Cu(phen)_2(H_2O)^{2+}$ cations and $Cu(phen)_2MF_6$ (phen = 1,10-phenanthroline; M = Zr, Hf) molecules.[40,41] In addition, the angle between the Cu atom and centroids of the ligands are quite different between the two unique cations, with Cation 1 being 151.41° and Cation 2 being 169.82° (Figure 5a). Notably, the angle in Cation 2 is distinctly larger than the rest of cations in this study. The τ_5 values of Cu cations in **4** are 0.55/0.46, indicating that the shape of the cations is largely distorted and cannot be described as

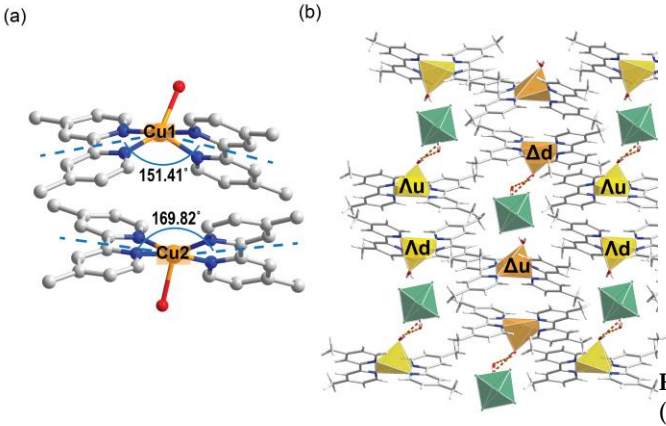

Figure 5. (a) Representation of the two Δ-$Cu(4dmbpy)_2(H_2O)^{2+}$ c are omitted. (b) The racemic layer of **4** view along the *b* axis. (c) red, grey, and white spheres represent Cu, N, O, C, and H atom resent Cu-centered cations with Λ- and Δ- configuration and Z represents hydrogen bonds.

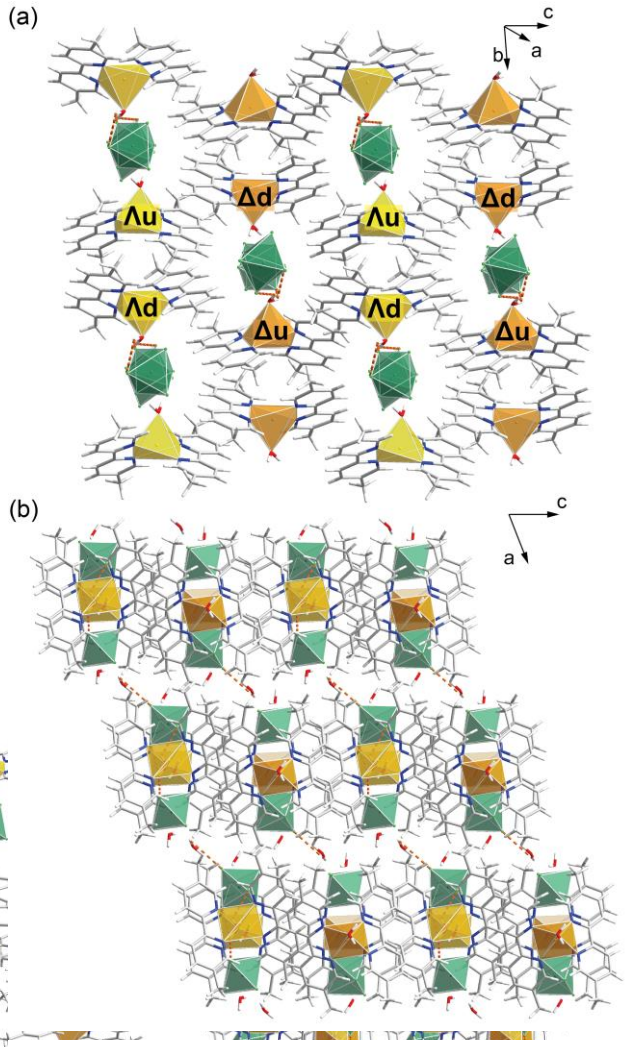

Figure 4. (a) Racemic layer of compound **2** in the *bc* plane. (b) Crystal structure of compound **2** view along the *b* axis. Orange, blue, red, grey, and white spheres represent Cu, N, O, C, and H atoms, respectively. Yellow, orange, and green polyhedra represent Cu-centered cations with Λ- and Δ- configuration and Zr-centered anions, respectively. The orange dashed line represents hydrogen bonds.

either a triangular bipyramid or a square pyramid. Interestingly, the second largest angle β is O1–Cu1–N3 for Cation 1 while it is N6–Cu2–N8 for Cation 2, suggesting that the bound water in Cation 1 is more tilted. Nevertheless, the distortion in the cations does not pose a large influence on the enantiomer stacking, and the Cu enantiomers still pack into Λd–Δu–Λd–Δu and Λu–Δd–Λu–Δd chains along the *c* axis (u = up and d = down describe the orientation of these cations along the *a* direction) via heterochiral *π*-*π* stacking interactions and extend into layers via homochiral *π*-*π* stacking interactions. Moreover, the pair of enantiomers with opposite handedness (Λu/Δd and Λd/Δu) are still related by an inversion center along the chain. The distortion in the cations leads to a tilt on the chain stacking, giving the β angle a value of 96.078(2)° (

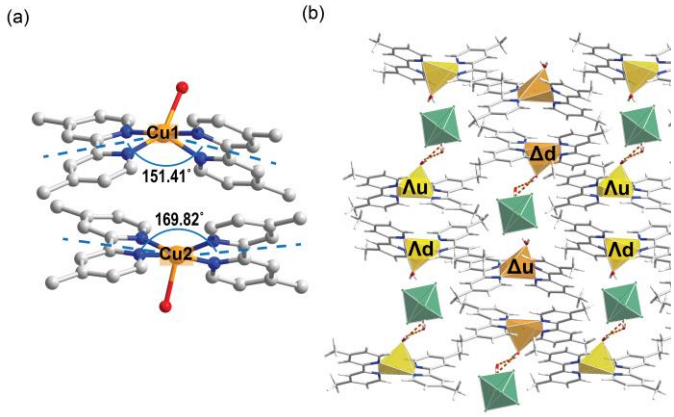

Figure 5b). Different from compound **1**, **2** and **3**, the two unique anions in **4** are not evenly distributed on the sides of the layers. In **4**, Anion 1 occupies the voids created by the adjacent racemic chains within the layer while Anion 2 is positioned between the layers. The uneven distribution of anion complicates the hydrogen bonding network wherein both anions form hydrogen bonds with Cation 1 but only Anion 1 forms hydrogen bonds with Cation 2. Despite the different hydrogen bonding schemes, the ZrF_6^{2-} octahedra are similar to those in **2**, with Zr—F bond lengths ranging from 1.972(2) to 2.0345(19) Å. The layers stack into three dimensions in an eclipsed manner through a linear intermolecular hydrogen bond network, where the free water molecules between the layers only form hydrogen bond with Anion 2 (

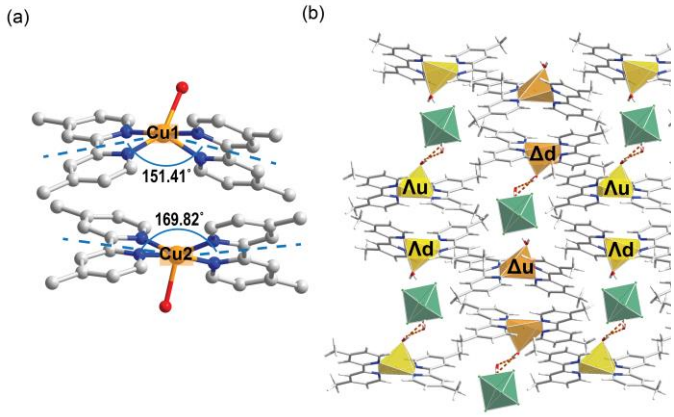

Figure 5c).

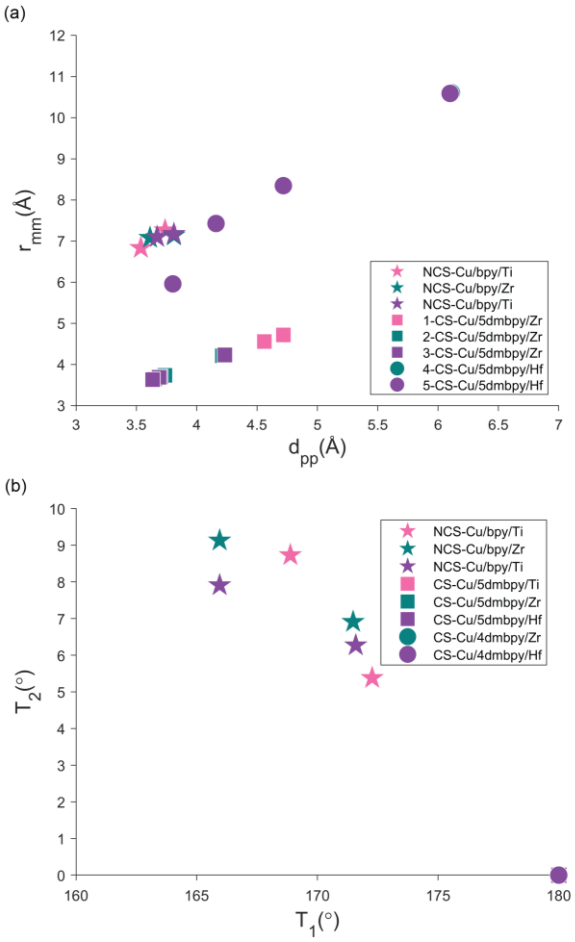

Figure 6. Summary of (a) *d*PP, *r*mm, (b) *T*1, and *T*2 parameters for heterochiral π–π stacking interactions in the reported NCS compounds and compounds **1-5**. The pink, green and purple squares and circles are eclipsed in (b).

Compound **5** has the formula $[Cu(4dmbpy)_2(H_2O)]_2[HfF_6]_2{\cdot}7H_2O$ and is isostructural to compound **4**. The cations in **5** are also distorted and tilted with the angle between the Cu atom and centroids of the ligands being 151.4/169.84° and τ_5 values being 0.55/0.47. The Hf—F bond lengths vary from 1.9668(19) to 2.0262(18) Å.

Structural Descriptors for *π*–*π* Interactions

Single crystal X-ray diffraction reveals three new structure types in compounds **1-5**. Unlike the reported NCS-Cu/bpy/M structure, all compounds in this work crystalize in CS space groups, even though they share similar packing motifs. To understand the nuance of packing patterns, we investigate the *π*–*π* stacking interactions between the adjacent Cu enantiomers in the reported NCS compounds and compounds **1-5** using the descriptors defined in the Methods section. The five descriptors, d_{PP}, *R*, r_{mm}, T_1, and T_2, depict the geometry of *π*–*π* stacking interactions between enantiomers in different aspects. The d_{PP} and *R* parameters describe the direct and normal distance between the interacting aromatic rings, respectively, while the r_{mm} parameter indicates the overlaps between the chelate–chelate stacking interactions. The two torsion angles, T_1, and T_2,

determine the orientation of the chelate rings and the relative direction of the interacting aromatic rings, respectively. A T_1 angle smaller than 90° corresponds to a *head-to-head* orientation, while a T_1 angle larger than 90° corresponds to a *head-to-tail* orientation. The absolute value of $|T_2|$ suggests the deviation between the direction of the interacting ligands.

The resulting descriptor values are provided in Table S3-5 and both heterochiral (along the chain direction) and homochiral (against the chain direction) π–π stacking interactions are examined. For each NCS-Cu/bpy/M compound, two unique heterochiral and two unique homochiral π–π stacking interactions are found. For each CS compound, four unique heterochiral and two unique homochiral π–π stacking interactions are found. Among the measured heterochiral π–π stacking interactions, the values of the *R* parameter vary little across different compounds and are all in a range of 3.221-3.725 Å, suggesting that the normal distance between the interacting aromatic rings does not change significantly between the NCS and CS compounds. In compounds **4** and **5**, d_{PP} and r_{mm} are around to 6.1 and 10.6 Å, respectively, which are significantly larger than the values in the rest of other compounds (Figure 6a). The deviation is due to the low symmetry and large distortion of the $Cu(4dmbpy)_2(H_2O)^{2+}$ complex, leading to an uneven spacing between the Cu enantiomers in the chain, as every other Cu enantiomer is closer to one neighbor and further away from the other (Figure S3). Interestingly, the extreme d_{PP} and r_{mm} values are only found in the racemic chains containing Cation 2 and it might be influenced by other secondary molecular forces such as hydrogen bonding. Among the measured homochiral π–π stacking interactions, the values of the *R*, d_{PP}, and r_{mm} parameters are in a range of 3.348-4.074, 3.815-4.453, and 2.188-4.206 Å with no distinct outlier.

The values of the T_1 and T_2 parameters found in the heterochiral π–π stacking interactions are in the range of 165-180° and 0-10°, respectively, suggesting that the chelate rings are in a *head-to-tail* orientation and both aromatic rings overlap along the chain (Figure 6b). Notably, the values of the T_1 and T_2 parameters are exactly 180° and 0° for all the CS compounds **1-5** while they vary in between 165.95 to 172.27° in the NCS-Cu/bpy/M compounds. This fact manifests a distinct nuance of the comparable packing patterns between CS and NCS compounds, in which the heterochiral π–π interactions are *parallel* between the adjacent pair of enantiomers with opposite handedness in the CS structures but are *nonparallel* in the NCS structure. For the homochiral π–π stacking interactions, the T_1 parameters and the T_2 parameters are in the range of 0.17-28.43° and of 3.01-19.55°, suggesting a *head-to-head* and *nonparallel* orientation. No obvious trend is found in the homochiral π–π stacking interactions.

Structural Descriptors for Racemic Chain Arrangement

To probe the nuance of chain arrangements between the NCS and CS compounds, we utilized the R_M and Φ descriptors and the results are summarized in Table S6-8. The R_M parameter describes the normal distance between the enantiomers with opposite handedness along the chains and the Φ parameter depicts the offset degree of the racemic chains. Regardless of the space group the compound crystallizes in, the chain of each structure features a zigzag pattern. The results of the R_M parameters give similar values in most of the compounds and the outlier appears in one of the chains compounds **4** and **5** (Figure S3). The large R_M values in this chain can be rationalized by the flat geometry of Cation 2, giving a distinct offset in the packing of the enantiomers. The results of the Φ parameters gives values ranging from 151.40 to 178.10°. It indicates the enantiomers in the chains are fluctuating in different levels. The chains that have the largest Φ parameters with a nearly linear shape is the chains containing Cu1 in compounds **2** and **3**. There is no clear trend to distinguish NCS and CS compounds based on the chain arrangement.

Discussion

Nonparallel π–π Interactions Break Local Inversion Symmetry between Racemates.

The analysis of structural descriptors for π–π interactions highlights a clear distinction between the NCS and CS racemic compounds, which is the stacking manner of racemic BBUs. In the CS structures, the ligands of enantiomorphic pairs stack in parallel while in the NCS structures they stack in nonparallel conformations (Figure 7). Moreover, the inversion center appears exactly in the center of the parallel heterochiral π–π interactions between the adjacent pair of enantiomers (eg: Δu-Cu1/Λd-Cu1) along the chain in the CS structures (Figure 7). Contrastingly, in the NCS structure, no symmetry element relates to the adjacent pair of enantiomers (eg: Δu-Cu2/Λd-Cu1) along the chain owing to the nonparallel heterochiral π–π stacking, and the enantiomers with opposite handedness (eg: Δd-Cu1/Λd-Cu1) are related by an *n* glide plane across the chains (Figure 7). The parallel heterochiral π–π stacking interactions in compounds **1-5** can be explained by the steric effect of the methyl groups on the ligands, in that the bulk methyl groups favors parallel stacking to minimize free volume.[19] Similar parallel heterochiral π–π packings were observed in racemic compounds with other methyl-substituted ligands and the aromatic ligand 1,10-phenanthroline, and an inversion center is always found between the racemates.[40,42,43] As a result, although the asymmetric unit of the discussed compounds contain equivalent BBUs, the BBUs are related by different symmetry elements, resulting in different extended structures. The racemic chains display a similar pattern but have different compositions between NCS and CS structures. In the NCS structure, two unique racemic BBUs are running along the chain, eg: Δu-Cu2—Λd-Cu1—Δu-Cu2—Λd-Cu1, but in the CS structures, the chain only contain one unique BBU, eg: Δu-Cu1—Λd-Cu1—Δu-Cu1—Λd-Cu1 (Figure 7).

While the current study details that parallel stacking interactions lead to a centrosymmetric arrangement of racemic motifs, and that nonparallel stacking interactions leads to a noncentrosymmetric arrangement of racemic motifs, it cannot be said that the occurrence of parallel or nonparallel stacking interactions defines the presence of an inversion center. It has yet to be observed by the authors if there are instances of parallel heterochiral π-π stacking interactions in NCS racemates—though in the case of the compounds this work, the nonparallel stacking interactions are necessary for inversion symmetry breaking. Furthermore, while in the CS compounds with parallel stacking interactions the inversion center was found between the enantiomorphic pair within the chain, this is not the only location that an inversion center can be located within the structure, or the only way the enantiomorphic pair can be related to one another.

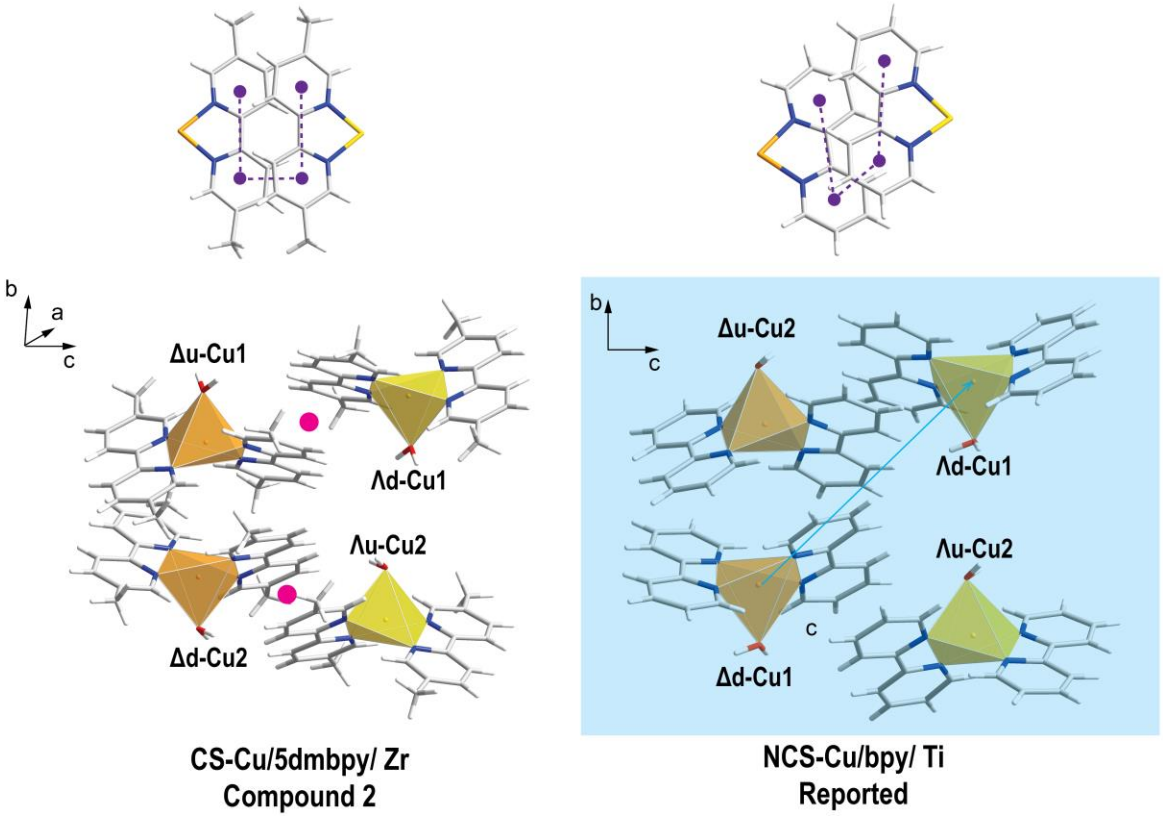

Figure 7. *Parallel* and *nonparallel* heterochiral π–π stacking interactions in NCS and CS compounds. The T_2 descriptor (top) and symmetry operations related the enantiomers with opposite handedness (bottom) are labeled. The pink circles and blue plane/arrow represent the inversion center and *n* glide, respectively.

Hydrogen Bonding Network Leads to Different Interlayer Structures.

Apart from the π–π stacking interactions, hydrogen bonding also plays a very important role in constructing the racemic structure, especially in the interlayer stacking. We analyzed the hydrogen bonding interactions across the discussed compounds and found that the geometry of the Cu enantiomer is strongly related to the local hydrogen bonding network. As shown in Figure S4, because of different distributions of free water, the MF_6^{2-} octahedra displays slightly different orientations across the NCS compounds and compounds **1**-**3**. It gives rise to a slight offset in the relative positions of the Cu enantiomers across the chain and a small tilt on the chain packing. The deviated hydrogen bonding network in compounds **4**-**5** derives from the unique voids created by the 4dmbpy ligands, which lead to the uneven distribution of the anions (Figure S5). The asymmetric anion distribution induces the large distortion of the $Cu(4dmbpy)_2(H_2O)^{2+}$ cations and thereby reduces the symmetry of the cations to C_1. The unique anions arrangements and linear hydrogen bonding network exclude an inversion center between the layers and the adjacent layers are related by a glide plane and screw axis in compounds **4**-**5**. While in compounds **1**-**3**, evenly distributed anion arrangements and intricate hydrogen bonding networks produce inversion symmetry between the layers (Figure 8). Note that although NCS compounds and compounds **1**-**3** present similarities in the anion arrangements and hydrogen bonding networks, the methyl group in compounds **1**-**3** enables a larger void and increased interlayer distance for the anions to align in a preferred orientation that minimizes the net dipole moment, so that the layers are packed through an inversion center other than a screw axis in NCS compounds (Figure 8).

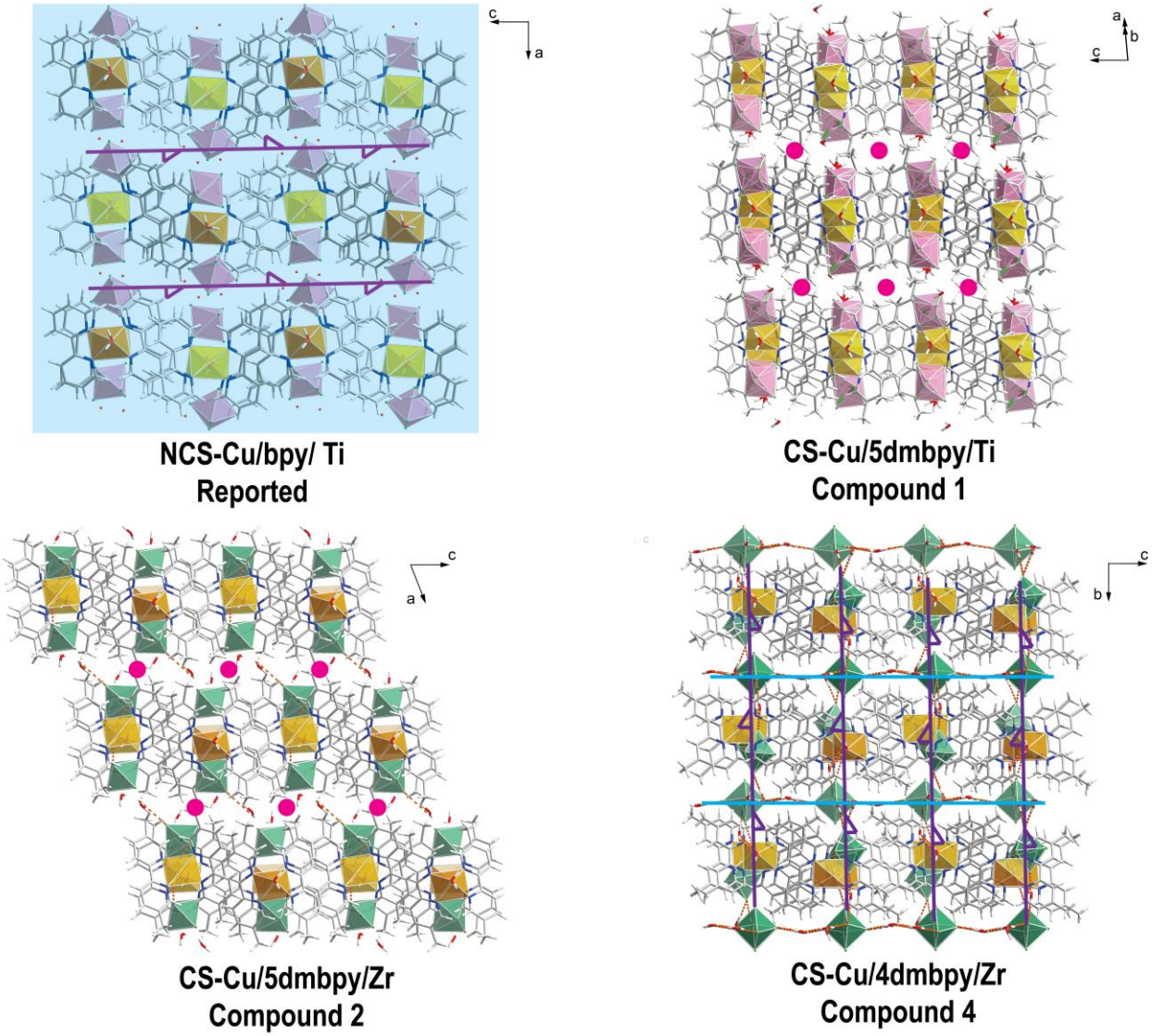

Figure 8. The interlayer architectures in the discussed compounds. Orange dash line represents hydrogen bonding. The blue, pink, and purple labels represent glide plane, inversion center, and screw axis, respectively.

Conclusion

In summary, we synthesized five new CS racemic compounds with dmbpy ligands and structurally analyzed their intermolecular forces in comparison to previously reported NCS racemic compounds. The structural descriptors have demonstrated that all CS compounds display parallel heterochiral π–π interactions between the adjacent enantiomers despite the difference in interlayer architecture, hydrogen bonding network, and cation geometry. In contrast, all heterochiral π–π interactions in the NCS compounds are nonparallel, which breaks the inversion center between the adjacent enantiomers. The parallel heterochiral π–π stacking in the compounds with dmbpy ligands can be explained by steric effects from the methyl group. Altogether, we demonstrate that nonparallel packing of ligands plays a very important role in breaking inversion symmetry between enantiomers and racemic BBUs which favor nonparallel packing have great potential to form NCS racemates.

Further, through the structural analysis of the five newly synthesized compounds and the comparison of these to the related NCS phases, common symmetry elements relating enantiomorphic pairs and their resulting space groups (Figure 1) have been identified. Ongoing work is focused on a comprehensive computational search for racemates in the NCS achiral crystal classes. Through this, we aim to unlock more secrets behind inversion symmetry breaking in racemates, which will provide further synthetic guides, such as desirable racemic BBUs, to target racemic materials with superior NCS properties. This goal aligns well with that outlined by A. F. Wells almost 70 years ago in 1956, *"to encourage the reader to think 'in three dimensions' so that he will come to regard the formation of three-dimensional arrangements of atoms in crystals as the logical results of the same processes that lead to the more familiar finite groups of atoms of ordinary chemical experience."*[44]

ASSOCIATED CONTENT

The Supporting Information is available free of charge on the ACS Publications website.

Additional characterization and analysis data (PDF)

Accession Codes

CCDC 2264645-2264649 contains the supplementary crystallographic data for this paper. These data can be obtained free of charge via www.ccdc.cam.ac.uk/data_request/cif, or by emailing data_request@ccdc.cam.ac.uk, or by contacting The Cambridge Crystallographic Data Centre, 12 Union Road, Cambridge CB2 1EZ, UK; fax: +44 1223 336033.

AUTHOR INFORMATION

Corresponding Author

* krp@northwestern.edu

Author Contributions

The manuscript was written through contributions of all authors.

Notes

The authors declare no competing financial interest.

ACKNOWLEDGMENT

This work was supported by fundings from the National Science Foundation (DMR-1904701). PSH thanks the Welch Foundation (Grant E-1457) and the National Science Foundation (DMR-2002319) for support. Single-crystal X-ray diffraction data were acquired at IMSERC at Northwestern University, which has received support from the Soft and Hybrid Nanotechnology Experimental (SHyNE) Resource (NSF ECCS-1542205), the State of Illinois, the International Institute for Nanotechnology (IIN), and the National Science Foundation (DMR-0521267). The authors thank Dr. C. D. Malliakas and Ms. C. Stern for experimental assistance.

REFERENCES

(1) Halasyamani, P. S.; Poeppelmeier, K. R. Noncentrosymmetric Oxides. *Chem. Mater.* **1998**, *10*, 2753.

(2) Kim, E.; Lee, D. W.; Ok, K. M. Centrosymmetric $[N(CH_3)_4]_2TiF_6$ vs. Noncentrosymmetric Polar $[C(NH_2)_3]_2TiF_6$: A Hydrogen-Bonding Effect on the out-of-Center Distortion of TiF_6 Octahedra. *J. Solid State Chem.* **2012**, *195*, 149.

(3) Eaton, D. F. Nonlinear Optical Materials. *Science* **1991**, *253*, 281.

(4) Weis, R. S.; Gaylord, T. K. Lithium Niobate: Summary of Physical Properties and Crystal Structure. *Appl. Phys. A* **1985**, *37*, 191.

(5) Ding, F.; Nisbet, M. L.; Yu, H.; Zhang, W.; Chai, L.; Halasyamani, P. S.; Poeppelmeier, K. R. Syntheses, Structures, and Properties of Non-Centrosymmetric Quaternary Tellurates $BiMTeO_6$ (M = Al, Ga). *Inorg. Chem.* **2018**, *57*, 7950.

(6) Welk, M. E.; Norquist, A. J.; Arnold, F. P.; Stern, C. L.; Poeppelmeier, K. R. Out-of-Center Distortions in D^0 Transition Metal Oxide Fluoride Anions. *Inorg. Chem.* **2002**, *41*, 5119.

(7) Gautier, R.; Gautier, R.; Chang, K. B.; Poeppelmeier, K. R. On the Origin of the Differences in Structure Directing Properties of Polar Metal Oxyfluoride $[MO_xF_{6-x}]^{2-}$ (x = 1, 2) Building Units. *Inorg. Chem.* **2015**, *54* , 1712.

(8) Donakowski, M. D.; Gautier, R.; Lu, H.; Tran, T. T.; Cantwell, J. R.; Halasyamani, P. S.; Poeppelmeier, K. R. Syntheses of Two Vanadium Oxide–Fluoride Materials That Differ in Phase Matchability. *Inorg. Chem.* **2015**, *54*, 765.

(9) Pinlac, R. A. F.; Stern, C. L.; Poeppelmeier, K. R. New Layered Oxide-Fluoride Perovskites: $KNaNbOF_5$ and $KNaMO_2F_4$ ($M = Mo^{6+}, W^{6+}$). *Crystals* **2011**, *1*, 3.

(10) Ding, F.; Nisbet, M. L.; Zhang, W.; Halasyamani, P. S.; Chai, L.; Poeppelmeier, K. R. Why Some Noncentrosymmetric Borates Do Not Make Good Nonlinear Optical Materials: A Case Study with $K_3B_5O_8(OH)_2$. *Inorg. Chem.* **2018**, *57*, 11801.

(11) Mutailipu, M.; Poeppelmeier, K. R.; Pan, S. Borates: A Rich Source for Optical Materials. *Chem. Rev.* **2021**, *121*, 1130.

(12) Ding, F.; Griffith, K. J.; Zhang, W.; Cui, S.; Zhang, C.; Wang, Y.; Kamp, K.; Yu, H.; Halasyamani, P. S.; Yang, Z.; Pan, S.; Poeppelmeier, K. R. $NaRb_6(B_4O_5(OH)_4)_3(BO_2)$ Featuring Noncentrosymmetry, Chirality, and the Linear Anionic Group BO_2^-. *J. Am. Chem. Soc.* **2023**, *145*, 4928.

(13) Yu, H.; Nisbet, M. L.; Poeppelmeier, K. R. Assisting the Effective Design of Polar Iodates with Early Transition-Metal Oxide Fluoride Anions. *J. Am. Chem. Soc.* **2018**, *140*, 8868.

(14) Ding, Q.; Liu, X.; Zhao, S.; Wang, Y.; Li, Y.; Li, L.; Liu, S.; Lin, Z.; Hong, M.; Luo, J. Designing a Deep-UV Nonlinear Optical Fluorooxosilicophosphate. *J. Am. Chem. Soc.* **2020**, *142*, 6472.

(15) Wu, C.; Lin, L.; Jiang, X.; Lin, Z.; Huang, Z.; Humphrey, M. G.; Halasyamani, P. S.; Zhang, C. $K_5(W_3O_9F_4)(IO_3)$: An Efficient Mid-Infrared Nonlinear Optical Compound with High Laser Damage Threshold. *Chem. Mater.* **2019**, *31*, 10100.

(16) Xiong, L.; Wu, L.-M.; Chen, L. A General Principle for DUV NLO Materials: π-Conjugated Confinement Enlarges Band Gap**. *Angewandte Chemie International Edition* **2021**, *60*, 25063.

(17) Zhang, Z.-P.; Liu, X.; Liu, X.; Lu, Z.-W.; Sui, X.; Zhen, B.-Y.; Lin, Z.; Chen, L.; Wu, L.-M. Driving Nonlinear Optical Activity with Dipolar 2-Aminopyrimidinium Cations in $(C_4H_6N_3)^+(H_2PO_3)^-$. *Chem. Mater.* **2022**, *34*, 1976.

(18) Mighell, A. D.; Himes, V. L.; Rodgers, J. R. Space-Group Frequencies for Organic Compounds. *Acta Cryst A* **1983**, *39*, 737.

(19) Brock, C. P.; Dunitz, J. D. Towards a Grammar of Crystal Packing. *Chem. Mater.* **1994**, *6*, 1118.

(20) Guerin, S.; O'Donnell, J.; Haq, E. U.; McKeown, C.; Silien, C.; Rhen, F. M. F.; Soulimane, T.; Tofail, S. A. M.; Thompson, D. Racemic Amino Acid Piezoelectric Transducer. *Phys. Rev. Lett.* **2019**, *122*, 047701.

(21) Gautier, R.; Norquist, A. J.; Poeppelmeier, K. R. From Racemic Units to Polar Materials. *Cryst. Growth Des.* **2012**, *12*, 6267.

(22) Guerin, S.; O'Donnell, J.; Haq, E. U.; McKeown, C.; Silien, C.; Rhen, F. M. F.; Soulimane, T.; Tofail, S. A. M.; Thompson, D. Racemic Amino Acid Piezoelectric Transducer. *Phys. Rev. Lett.* **2019**, *122*, 047701.

(23) Nisbet, M. L.; Pendleton, I. M.; Nolis, G. M.; Griffith, K. J.; Schrier, J.; Cabana, J.; Norquist, A. J.; Poeppelmeier, K. R. Machine-Learning-Assisted Synthesis of Polar Racemates. *J. Am. Chem. Soc.* **2020**, *142*, 7555.

(24) McNaught, A. D.; Wilkinson, A. *Compendium of Chemical Terminology*, 2nd ed.; Wiley, 1994.

(25) Fábián, L.; Brock, C. P. A List of Organic Kryptoracemates. *Acta Cryst B* **2010**, *66*, 94.

(26) Clevers, S.; Coquerel, G. Kryptoracemic Compound Hunting and Frequency in the Cambridge Structural Database. *CrystEngComm* **2020**, *22*, 7407.

(27) Dalhus, B.; Görbitz, C. H. Non-Centrosymmetric Racemates: Space-Group Frequencies and Conformational Similarities between Crystallographically Independent Molecules. *Acta Cryst B* **2000**, *56*, 71572.

(28) Moore, J. S.; Lee, S. Crafting Molecular Based Solids. *Chemistry and Industry (London)* **1994**, *14*, 556.

(29) Breu, J.; Domel, H.; Stoll, A. Racemic Compound Formation versus Conglomerate Formation with $[M(Bpy)_3](PF_6)_2$ (M = Ni, Zn, Ru); Molecular and Crystal Structures. *European Journal of Inorganic Chemistry* **2000**, *2000*, 2401.

(30) Potočňák, I.; Burčák, M.; Baran, P.; Jäger, L. Low-Dimensional Compounds Containing Cyano Groups. XI. Preparation, Crystal Structure and Properties of Two Copper(II) Dicyanamide Complexes with PF_6^- Anions. *Transition Met Chem* **2005**, *30*, 889.

(31) Zhu, M.; Peng, J.; Pang, H.-J.; Zhang, P.-P.; Chen, Y.; Wang, D.-D.; Liu, M.-G.; Wang, Y.-H. A New 3D Transition-Metal Complex-Templated Framework Based on Wells–Dawson Polyoxometalate and Copper(I)–Pyrazine Moieties. *Inorganica Chim. Acta* **2011**, *370*, 260.

(32) Guo, K. K. Experimental Crystal Structure Determination. *CSD Communication* **2020**.

(33) Harrison, W. T. A.; Nenoff, T. M.; Gier, T. E.; Stucky, G. D. Tetrahedral-Atom 3-Ring Groupings in 1-Dimensional Inorganic Chains: Beryllium Arsenate Hydroxide Hydrate ($Be_2AsO_4OH{\cdot}4H_2O$) and Sodium Zinc Hydroxide Phosphate Hydrate ($Na_2ZnPO_4OH{\cdot}7H_2O$). *Inorg. Chem.* **1993**, *32*, 2437.

(34) CrysAlisPRO, Oxford Diffraction /Agilent Technologies UK Ltd, Yarnton, England.

(35) Sheldrick, G. M. *SHELXTL*, version 6.12.; Bruker Analytical X-ray Systems, Inc.: Madison, WI, 2000.

(36) Dolomanov, O. V.; Bourhis, L. J.; Gildea, R. J.; Howard, J. a. K.; Puschmann, H. OLEX2: A Complete Structure Solution, Refinement and Analysis Program. *J Appl Cryst* **2009**, *42*, 339.

(37) Spek, A. PLATON, A Multipurpose Crystallographic Tool. *J. Appl. Cryst.* **1988**, *21*, 983.

(38) Petrović, P. V.; Janjić, G. V.; Zarić, S. D. Stacking Interactions between Square-Planar Metal Complexes with 2,2′-Bipyridine Ligands. Analysis of Crystal Structures and Quantum Chemical Calculations. *Cryst. Growth Des.* **2014**, *14*, 3880.

(39) Addison, A. W.; Rao, T. N.; Reedijk, J.; Rijn, J. van; Verschoor, G. C. Synthesis, Structure, and Spectroscopic Properties of Copper(II) Compounds Containing Nitrogen–Sulphur Donor Ligands; the Crystal and Molecular Structure of Aqua[1,7-Bis(N-Methylbenzimidazol-2′-Yl)-2,6-Dithiaheptane]Copper(II) Perchlorate. *J. Chem. Soc., Dalton Trans.* **1984**, *7*, 1349.

(40) Nisbet, M. L.; Wang, Y.; Poeppelmeier, K. R. Symmetry-Dependent Intermolecular π–π Stacking Directed by Hydrogen Bonding in Racemic Copper-Phenanthroline Compounds. *Cryst. Growth Des.* **2021**, *21*, 552.

(41) Melnic, E.; Coropceanu, E. B.; Kulikova, O. V.; Siminel, A. V.; Anderson, D.; Rivera-Jacquez, H. J.; Masunov, A. E.; Fonari, M. S.; Kravtsov, V. Ch. Robust Packing Patterns and Luminescence Quenching in Mononuclear $[Cu(II)(Phen)_2]$ Sulfates. *J. Phys. Chem. C* **2014**, *118*, 30087.

(42) Wang, Y.; Nisbet, M. L.; Poeppelmeier, K. R. Crystal Structures of Two Copper(I)–6,6′-Dimethyl-2,2′-Bipyridyl (Dmbpy) Compounds, $[Cu(Dmbpy)_2]_2[MF_6]{\cdot}xH_2O$ (M = Zr, Hf; x = 1.134, 0.671). *Acta Cryst E* **2021**, *77*, 819.

(43) Wang, Y.; Fukuda, M.; Nikolaev, S.; Miyake, A.; Griffith, K. J.; Nisbet, M. L.; Hiralal, E.; Gautier, R.; Fisher, B. L.; Tokunaga, M.; Azuma, M.; Poeppelmeier, K. R. Two Distinct Cu(II)–V(IV) Superexchange Interactions with Similar Bond Angles in a Triangular "CuV_2" Fragment. *Inorg. Chem.* **2022**, *61*, 10234.

(44) Wells, A. F. *The Third Dimension in Chemistry.*; Clarendon Press.

Table of Contents: